The change in the conductivity of seawater after catalysts addition

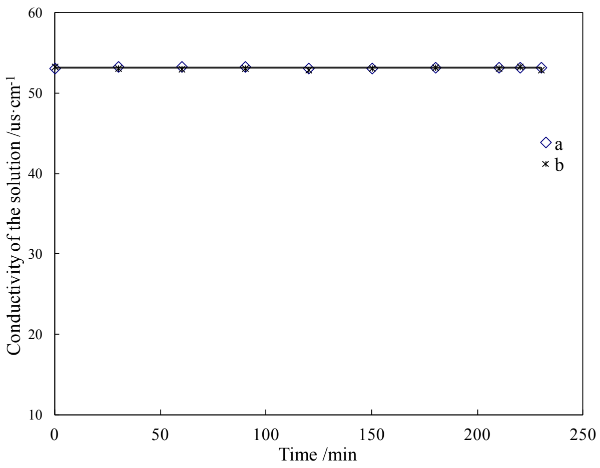

Figure S1 Dependences of conductivity of seawater on time after photocatalysts addition a. TiO_2-GO; b. TiO_2-RGO-$A_{1.5}$

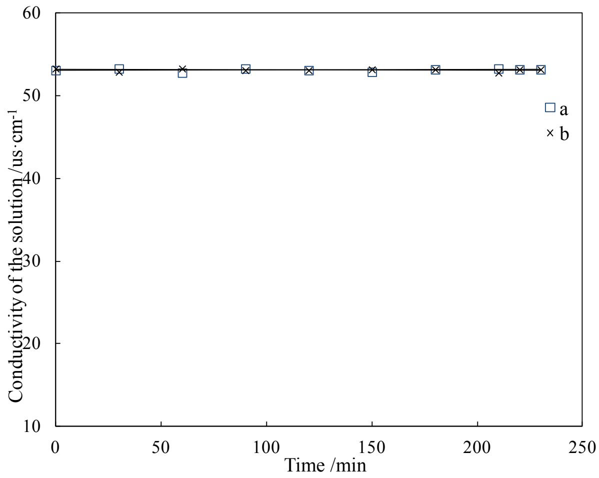

Figure S2 Dependences of conductivity of seawater on time after photocatalysts addition a. P25; b. SiO_2-TiO_2 (1.5mL of water in ALNS preparation)

The measurement of phenol in seawater or water

To avoid the disturbance of salt ions in seawater, 4-Aminoantipyrine spectrophotometric method, instead of HPLC methods in many literatures, was employed to measure the phenol concentration in seawater. Figure S3 first listed the standard curve of phenol in seawater by spectrophotometer using 4-aminoantipyrine spectrophotometric method. For reference, the standard curve of phenol in water was also listed in Figure S3.

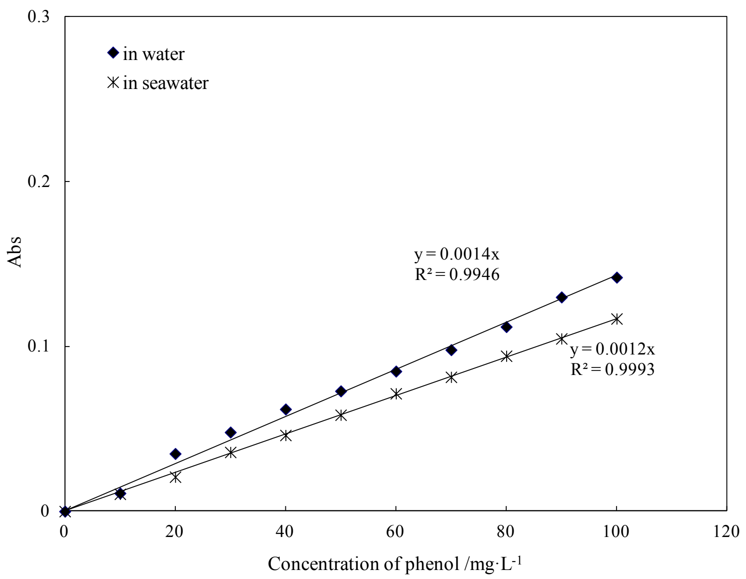

Figure S3 The standard curve of phenol in seawater and water measured by spectrophotometer (Wavelength 510 nm)

From Figure S3, the linear relationship between phenol concentration and absorbance was very good both in seawater and in pure water, which suggested that 4-aminoantipyrine spectrophotometric method was suitable for measuring the change in the photodegradation for phenol in our experiments. In addition, the slope of the two standard curves in Figure S4 was very close, which meant the salt ions showed small effects on the absorbance of phenol.

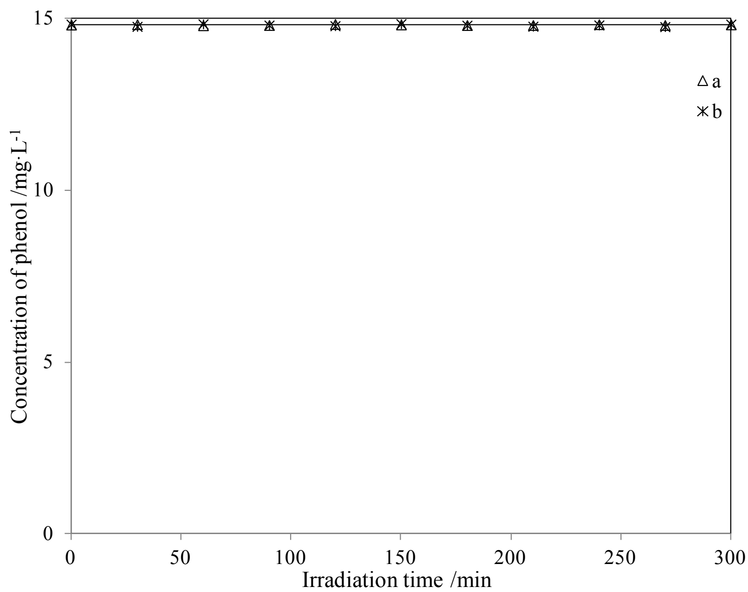

Figure S4 The blank degradation experiments of phenol illuminated under 4 W UV lamp

a. water; b. seawater

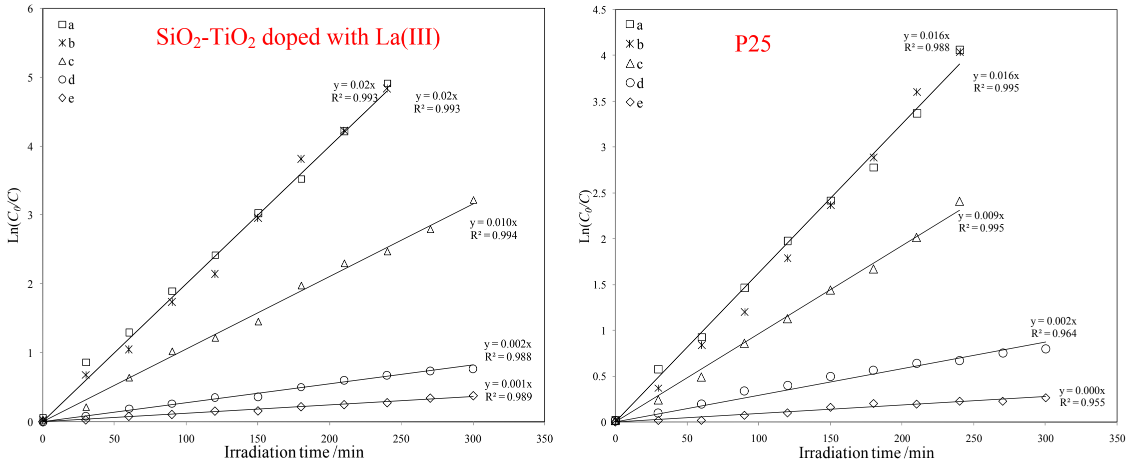

Figure S5 Degradation of phenol with different initial concentrataion by two catalysts in seawater

The initial concentration of phenol (/mg·L^{-1}): a. 5; b. 10; c. 15; d. 20; e. 25

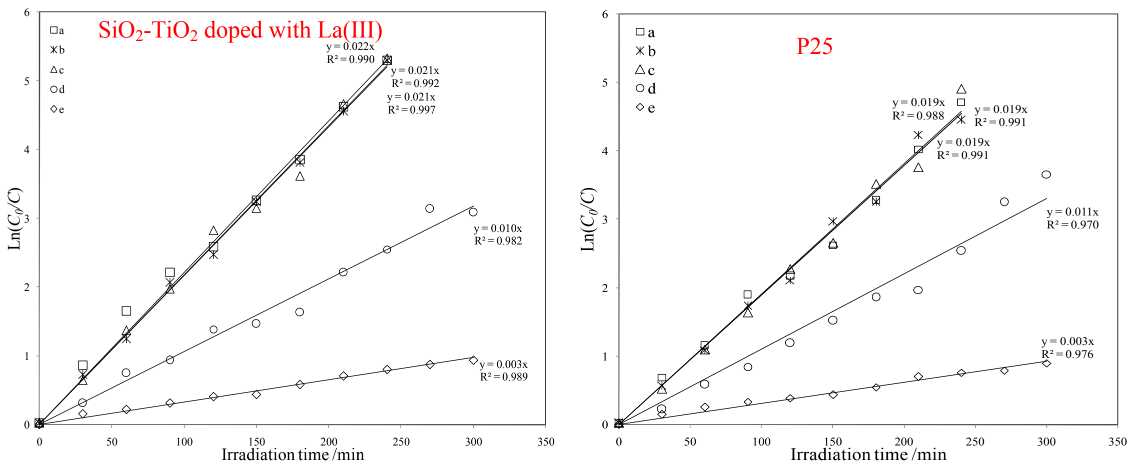

Figure S6 Degradation of phenol with different initial concentrataion by two catalysts in water

The initial concentration of phenol (/mg·L^{-1}): a. 5; b. 10; c. 15; d. 20; e. 25

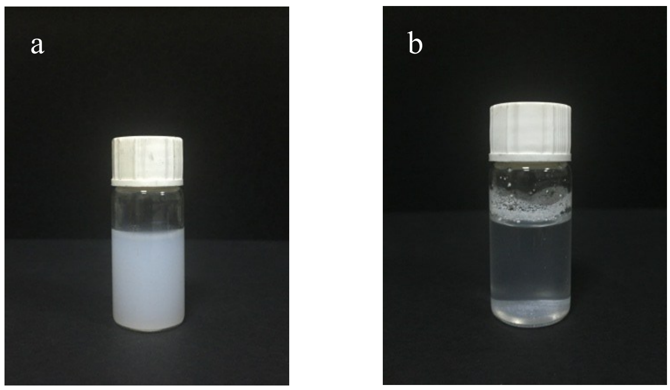

Figure S7 Digital photographs of the dispersion of La^{3+} doped SiO_2-TiO_2 in seawater

a. La^{3+} doped SiO_2-TiO_2 before solvothermal treatment; b. La^{3+} doped SiO_2-TiO_2 after solvothermal treatment

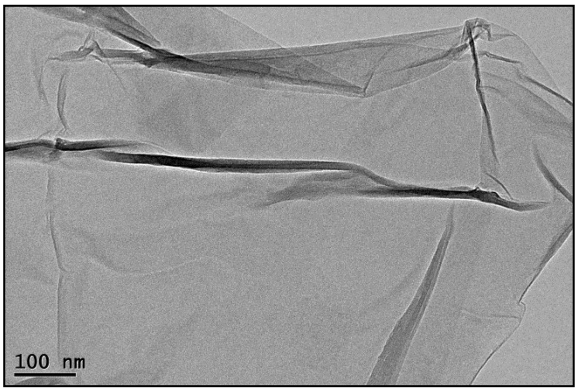

Figure S8 TEM images of Red-GO samples

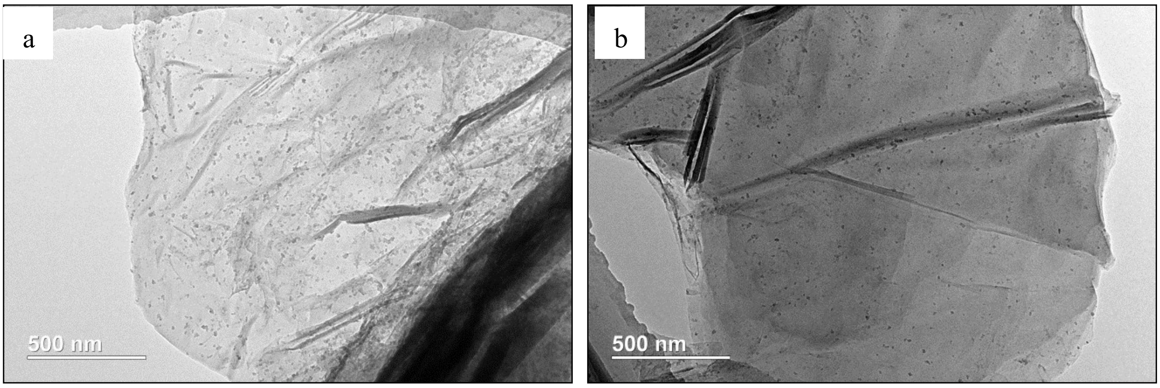

Figure S9 TEM images of two GO-TiO_2 before solvothermal treatment

a. GO-TiO_2 by ALNS; b. GO-TiO_2 doped with La^{3+} by ALNS

(1.5 mL of water in preparation)

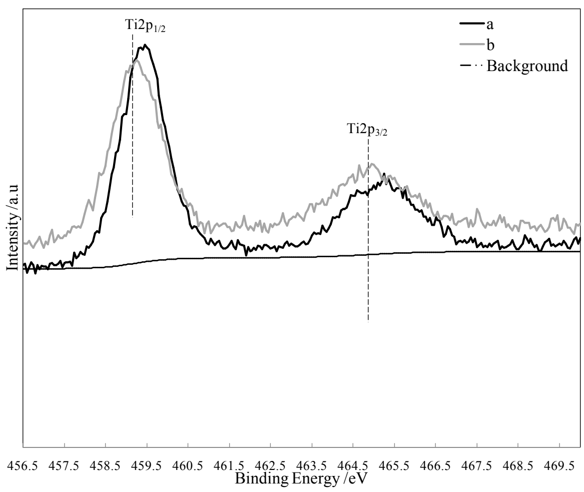

Figure S10 XPS profiles of Ti2p in two Red-GO-TiO_2 catalysts

a. Red-GO-TiO; b. La^{3+} doped Red-GO-TiO_2

Figure S11 Digital photographs of the dispersion of GO-TiO_2 and Red-GO-TiO_2 in seawater

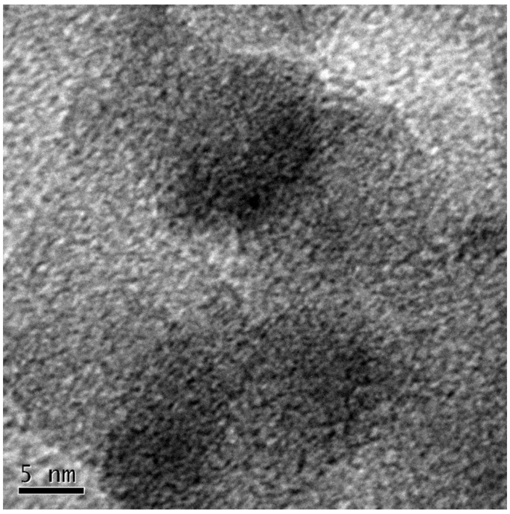

Figure S12 HRTEM images of GO-TiO_2 before solvothermal treatment

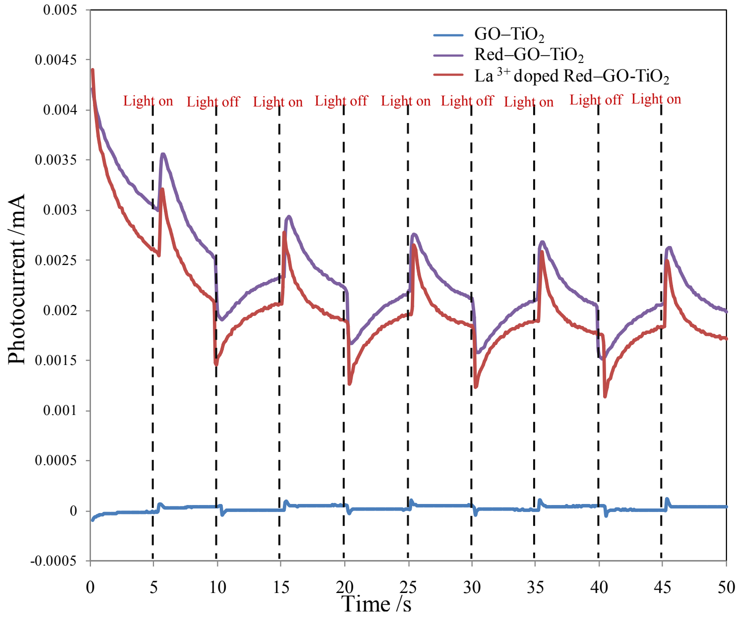

Figure S13 Photocurrent response of different photocatalysts

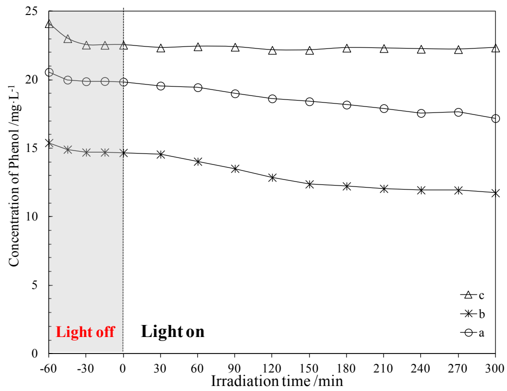

Figure S14 Photodegradation of different phenol concentrations using GO–TiO_2

The initial phenol concentration in seawater (/mg•L^{-1}): a. 15; b. 20; c. 25

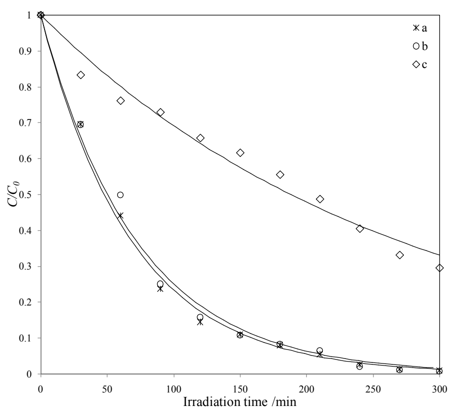

Figure S15 Degradation curves using Red–GO–TiO_2

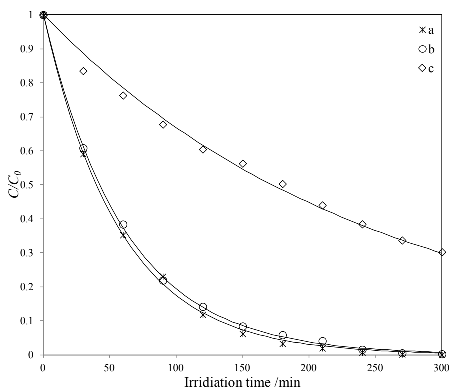

Figure S16 Degradation curves using La^{3+} doping Red–GO–TiO_2

The initial phenol concentration in seawater (/mg•L^{-1}): a. 15; b. 20; c. 25

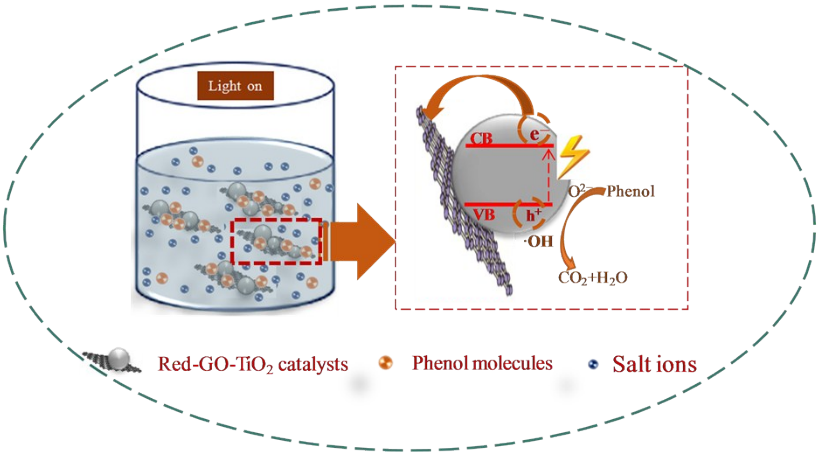

Scheme S1 The mechanism scheme on photodegradation process for phenol in seawater by Red-GO-TiO_2 with or without doping